

# Experimental study of self-trapping in capillary discharge guided laser wakefield acceleration\*

K. Nakamura, E. Esarey, C. G. R. Geddes, A. J. Gonsalves, W. P. Leemans<sup>†</sup>, C. Lin, D. Panasencko, C. B. Schroeder, and C. Toth, LBNL, Berkeley, CA 94720, USA

## Abstract

Laser wakefield acceleration experiments were carried out using hydrogen-filled capillary discharge waveguides. For a 33 mm long, 300  $\mu\text{m}$  capillary, parameter regimes with high energy electron beams (up to 1 GeV) and stable 0.5 GeV were found. In the high energy regime, the electron beam peak energy was correlated with the number of trapped electrons. For a 15 mm long, 200  $\mu\text{m}$  diameter capillary, quasi-monoenergetic e-beams up to 300 MeV were observed. By de-tuning discharge delay from optimum guiding performance, self-trapping was found to be stabilized.

## INTRODUCTION

Laser wakefield accelerators (LWFAs) [1] have demonstrated high field gradients, up to hundreds of GV/m, and the production of quasi-monoenergetic electron beams (e-beams) with energies of the order of 100 MeV in just a few millimeters [2, 3, 4]. Recently, by using a hydrogen-filled capillary discharge waveguide, LWFAs at up to a GeV have been realized at Lawrence Berkeley National Laboratory (LBNL) [5, 6]. In this scheme, intense laser pulses were guided over a distance 10 times the Rayleigh range by a preformed plasma channel with sufficiently low density to reduce energy gain limitations imposed by diffraction and dephasing [1]. During the laser plasma interaction, electrons were self-trapped from the background plasma, and accelerated up to the GeV level.

In the first generation of the capillary discharge guided LWFA experiments, accelerator performance was found to be quite sensitive and to exhibit a complicated interdependence on input laser and plasma parameters, such as the delay between the onset of the discharge current and arrival of the laser beam (discharge delay  $t_d$ ), the estimated on-axis plasma density  $n_0$  [7], and the peak laser power  $P$ . Electron beams with energies of 1 GeV were obtained in a 33 mm long, 300  $\mu\text{m}$  diameter capillary for  $P \sim 42$  TW and  $n_0 \simeq 4.3 \times 10^{18} \text{ cm}^{-3}$ . Although 1 GeV beam generation was not stable, a statistical analysis did show a parameter regime where 0.5 GeV e-beams were produced with improved stability by tightly controlling the input parameters for a 33 mm long, 225  $\mu\text{m}$  diameter capillary.

In order to design the next generation apparatus for stable production of higher quality e-beams, it is critical to untangle the interdependence of input laser and plasma parameters, which requires further parameter exploration and

analysis. In this paper, we report a performance analysis of the capillary discharge guided LWFA using a 33 mm long, 300  $\mu\text{m}$  diameter and a 15 mm long, 200  $\mu\text{m}$  diameter capillary. Experiments varying capillary length give insight into the physics of the capillary discharge guided LWFA.

## EXPERIMENTAL SETUP

The schematic of the experimental setup is shown in Fig. 1. The laser that was utilized was a 10 Hz Ti:Al<sub>2</sub>O<sub>3</sub> system of the LOASIS facility at LBNL. The laser beam was focused by a  $f/25$  off-axis parabolic mirror providing a typical focal spot size of  $r_0 \simeq 25 \mu\text{m}$  that contains 60% of the laser energy. Here, a Gaussian transverse profile of  $I = I_0 \exp(-2r^2/r_0^2)$  is assumed. Full energy and optimum compression gives  $P = 43$  TW,  $\tau_{in} \simeq 40$  fs full width half maximum (FWHM) intensity, calculated peak intensity  $I_0 = 2P/\pi r_0^2 \simeq 2.6 \times 10^{18} \text{ W/cm}^2$ , and a normalized vector potential  $a_0 \simeq 8.6 \times 10^{-10} \lambda[\mu\text{m}] I^{1/2} [\text{W/cm}^2] \simeq 1.1$ .

The capillary waveguide was laser-machined in sapphire plates. Hydrogen gas was introduced into the capillary using two gas slots as shown in Fig. 1(inset). A discharge was struck between electrodes located at each end of the waveguide, using a high voltage pulsed power supply with a 4 nF capacitor charged to between 15 and 22 kV. Measurements showed that a fully ionized, approximately parabolic channel was formed on axis [7]. This fully ionized feature was also confirmed by the absence of ionization induced blueshifting of the transmitted laser spectrum when a low power ( $< 0.2$  TW) laser pulse was guided.

The electron beams generated were characterized by an electron spectrometer providing a single-shot spectrum of 0.01 GeV to 0.14 GeV (bottom view) and 0.17 GeV to 1.1 GeV (forward view) [8]. The total number of elec-

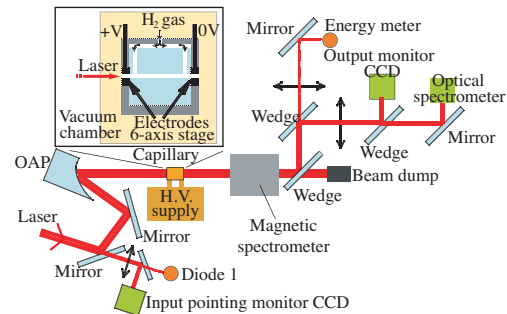


Figure 1: Schematic diagram of the experimental setup. The detailed description of the electron spectrometer can be found in Ref. [8].

\* Work supported by DOE grant DE-AC02-05CH11231, and DARPA

<sup>†</sup> wpleemans@lbl.gov

trons was obtained from the intensity on the scintillating screen, which was cross-calibrated against an integrating current transformer (ICT) at the Advanced Light Source, LBNL. The magnetic spectrometer allowed simultaneous measurement of the laser pulse and e-beam due to its large gap. The laser energy was monitored both before and after the interaction to evaluate the guiding efficiency and guided beam quality. The laser output spectrum was measured by a broadband optical spectrometer which covers a wavelength range of 320 to 1000 nm in a single shot.

## RESULTS

In 2006, generation of e-beams with energies of 1 GeV was reported for a 33 mm long, 300  $\mu\text{m}$  diameter capillary with three gas slots [5, 6]. Similarly to these results, a parameter regime where e-beams with energies of up to 1 GeV were produced was found here for a 33 mm long, 300  $\mu\text{m}$  diameter capillary with two gas slots. Representative single shot e-beam spectra are shown in Fig. 2(a)-(c). The plasma density was  $n_0 \sim 5.3 \times 10^{18} \text{ cm}^{-3}$ , the laser parameters were 1.5 J (86 mJ rms), 46 fs ( $a_0 \sim 0.93$ ), applied voltage was 18 kV, and the discharge delay was  $t_d \sim 580$  ns. In this parameter regime, 51 shots were taken, and 37 shots produced electrons above 400 MeV. The mean peak energy was 713 MeV, and mean charge was 6 pC. Since e-beams were often observed with a low energy tail in this regime, electrons with energy above 400 MeV were taken into account for the analysis. The mean laser transmission was 65%.

The peak energy and maximum energy versus total charge for 33 mm long, 300  $\mu\text{m}$  diameter capillary are shown in Fig. 2(d). The peak energy showed clear de-

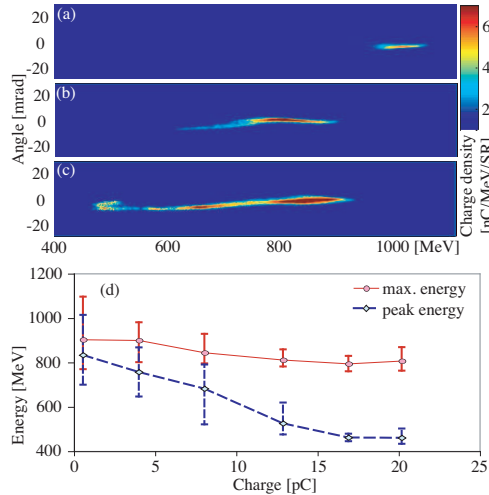


Figure 2: (a)-(c) Representative single shot e-beam spectra, (d) the peak energy and maximum energy versus charge for the 33 mm long, 300  $\mu\text{m}$  diameter capillary. (The plasma density was  $\sim 5.3 \times 10^{18} \text{ cm}^{-3}$ , the laser parameters were 1.5 J–46 fs, applied voltage was 18 kV, and the discharge delay was  $\sim 580$  ns.)

pendence on the charge, while the maximum energy was somewhat insensitive to charge. There are several possible scenarios. The trapped electron beam produces a wakefield which can partly cancel the wakefield generated by the laser pulse (beam loading effect). In the case of heavy beam loading, self-trapping can be stopped, and the tail of the electron beam sees lower accelerating field while the head sees maximum field, introducing energy spread to the electron beam. If beam loading is negligible, self-trapping can occur over a longer period of time, and these higher charge beams may be trapped over a larger phase region in the plasma wave, resulting in a larger energy spread. To produce high quality e-beams in a reproducible manner, controlling the amount, duration, and the location of trapped electrons will be critical.

Also found with this capillary was stable generation of quasi-monoenergetic 460 MeV beams (shown in Fig. 3) for plasma density  $n_0 \sim 3.4 \times 10^{18} \text{ cm}^{-3}$ , and laser parameters 1.5 J (36 mJ rms), 46 fs ( $a_0 \sim 0.93$ ). Applied voltage was 25 kV, and the discharge delay  $t_d \sim 680$  ns (with 0.9 ns rms jitter). In this parameter regime, 24 shots were taken, and all 24 shots produced electrons with mean charge 2.6 pC (2.0 pC rms), mean peak energy 458 MeV (24 MeV rms), and mean energy spread 4% rms. Applying longer discharge delay and higher voltage than the high energy regime resulted in stabilizing self-trapping and acceleration to somewhat lower electron energy.

In experiments using a 15 mm long, 200  $\mu\text{m}$  diameter capillary, the guiding performance and e-beam generation showed clear dependence on the discharge delay. The input laser parameters were 0.9 J (36 mJ rms), 41 fs ( $a_0 \sim 0.8$ ), and the plasma density was  $2.5$  or  $3.7 \times 10^{18} \text{ cm}^{-3}$ . Shown in Fig. 4(a) are the discharge delay dependence of several laser spectra bins. The center is defined as the light within the frequency bandwidth of  $770 \leq \lambda \leq 835$  nm, and 100% of incident light was within this band. The red (blue) shift is defined as  $835 < \lambda < 1000$  nm ( $320 < \lambda < 770$  nm). For relatively short discharge delay ( $t_d < 130$  ns), significant red-shift and moderate blue-shift were observed, consistent with the laser pulse modulation and energy deposition onto the plasma via wakefield generation [1]. For

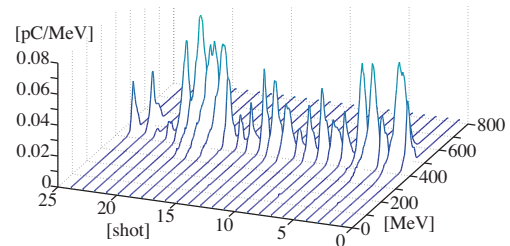


Figure 3: Single shot spectra of 24 consecutive shots for the 33 mm long, 300  $\mu\text{m}$  diameter capillary. The plasma density was  $\sim 3.4 \times 10^{18} \text{ cm}^{-3}$ , the laser parameters were 1.5 J–46 fs, applied voltage was 25 kV, and the discharge delay was  $\sim 680$  ns.

longer discharge delay ( $t_d > 130$  ns), the optical spectrum exhibited significant blue-shift as well as red-shift, and the transmission efficiency dropped.

The probability of observing any e-beam on the electron spectrometer vs.  $t_d$  is shown in Fig. 4(b) by dashed lines. For  $n_0 \sim 2.5 \times 10^{18} \text{ cm}^{-3}$ , no electron beams were observed for  $t_d < 110$  ns and transmission efficiency was high ( $> 80\%$ ). This suggests that, although a wakefield was generated based on the observation of significant red-shift, it was not large enough to trap background electrons. Electron beams were observed for longer discharge delay, along with a drop in transmission efficiency and enhanced blue-shift. For e-beams properties, relatively high energy ( $\sim 300$  MeV), low charge ( $< 10$  pC) quasi-monoenergetic e-beams were observed with shorter discharge delay while broadband high charge ( $\sim 100$  pC) beams were observed with longer delay. Note that by using higher density plasma ( $n_0 \sim 3.7 \times 10^{18} \text{ cm}^{-3}$ ), e-beams were observed for shorter discharge delay without significant blue shift in transmitted optical spectrum.

Several mechanisms could be responsible for the enhancement of blueshifting, laser transmission loss, and electron trapping observed for longer discharge delay. For

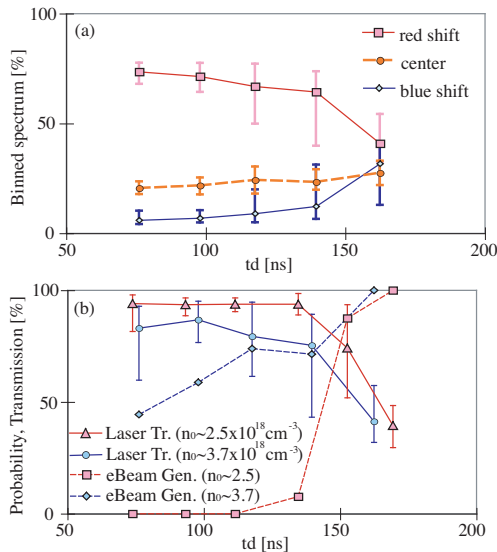


Figure 4: Results for 15 mm long, 200  $\mu\text{m}$  diameter capillary. (a) Binned transmitted optical spectrum versus discharge delay for plasma density  $\sim 2.5 \times 10^{18} \text{ cm}^{-3}$ . The center is defined as the light within the frequency bandwidth of  $770 \leq \lambda \leq 835$  nm. The red (blue) shift is defined as  $835 < \lambda < 1000$  nm ( $320 < \lambda < 770$  nm). (b) Transmission efficiency of laser pulses [solid line, triangles (circles) for  $n_0 \sim 2.5(3.7) \times 10^{18} \text{ cm}^{-3}$ ], and the probability of e-beam observation on the electron spectrometer [dashed line, squares (diamonds) for  $n_0 \sim 2.5(3.7) \times 10^{18} \text{ cm}^{-3}$ ] versus discharge delay. For both figures, the input laser parameters were 0.9 J and 41 fs. A total of 80 shots were taken for each plasma density. Bars show minimum and maximum points.

longer discharge delay, the degree of ionization, depth of the plasma channel, and plasma density decrease. It has also been suggested that the amount of discharge-ablated material interacting with the laser pulse increased [9]. For a substantial amount of laser pulse energy to be blueshifted by ionization requires the peak intensity of the laser pulse to be within an order of magnitude of the ionization intensity of the ion species with which the pulse interacts. In the case of hydrogen this is  $10^{14} - 10^{15} \text{ W/cm}^2$ , several orders of magnitude lower than the intensity of the laser in the channel. Ablated materials (e.g., aluminum, oxygen) have higher ionization thresholds, and the deteriorated channel may lead to laser ablation of the capillary wall. The reduced laser transmission was likely due to ionization and/or laser leakage from the degraded channel. Recent study also suggested the interaction with a partially ionized plasma could assist self-trapping [10]. Discharge-ablated materials drifting to the axis before the arrival of the laser could contribute to this process due to its transit time. Note that laser-ablated materials could not contribute to this process. Another possible reason for increased trapping is increase of the on-axis plasma density due to the deterioration of the channel. Although the degree of ionization decreases for longer discharge delay, the laser pulse was strong enough to ionize hydrogen.

## SUMMARY

In summary, relativistic electron beam generation via a capillary discharge guided LWFA was studied by using 15 mm long, 200  $\mu\text{m}$  diameter and 33 mm long, 300  $\mu\text{m}$  diameter capillaries. Generation of quasi-monoenergetic e-beams up to 1 GeV was observed from the the 33 mm long capillary, and up to 300 MeV was observed from the 15 mm long capillary. By using longer discharge delay, self-trapping was stabilized. This regime could be used to design a stable self injection capillary discharge guided LWFA. While reproducible beams have been observed in tightly controlled parameter regime, a controlled mechanism for injection will be important to enhance the LWFA performance.

## REFERENCES

- [1] E. Esarey, *et al.*, IEEE Trans. Plasma Sci. **24**, 252 (1996).
- [2] S. Mangles, *et al.*, Nature **431**, 535 (2004).
- [3] C. G. R. Geddes, *et al.*, Nature **431**, 538 (2004).
- [4] J. Faure, *et al.*, Nature **431**, 541 (2004).
- [5] W. P. Leemans, *et al.*, Nature Physics **2**, 696 (2006).
- [6] K. Nakamura, *et al.*, Phys. Plasmas **14**, 056708 (2007).
- [7] A. J. Gonsalves, *et al.*, Phys. Rev. Lett. **98**, 025002 (2007).
- [8] K. Nakamura, *et al.*, Rev. Sci. Instrum. **79**, 053301 (2008).
- [9] A. J. Gonsalves, Ph.D. thesis, University of Oxford (2006).
- [10] T. P. Rowlands-Rees, *et al.*, Phys. Rev. Lett. **100**, 105005 (2008).